ANY CHANCE OF CONTROLLING CRYSTALLIZATION BEHAVIOR OF MOLD FLUXES? NEW INSIGHTS.

C.Righi, R.Carli and V.Ghilardi
Prosimet SpA, Via Rodi 10, 24040 Filago (BG) Italy. Phone: +39-035-4938-971.
FAX: +39-035-4938-973. WEB: prosimet.com E-MAIL: prostech@tin.it

---

Abstract

Crystallization of MnO-doped and un-doped mold fluxes at different cooling rates was investigated to study peculiar chemical-physical effects induced by this transition metal oxide. By DTA analysis relationship between onset of crystallization and cooling rate was evidenced.
Crystallization temperatures calculated by extrapolation for cooling rates approaching zero were found quite similar to equilibrium break temperatures determined with high temperature rotational viscosimetry.

1.0 Introduction

Control of crystallization within a mold flux is a key factor for optimal operations of steel continuous casting. In a previous work, it has been shown that mold flux crystallization behavior can be controlled for some extent by doping the flux with suitable transition metal oxide [1]. It has been found that the most suitable doping compound contains MnO [2]. Extent of MnO doping has proved to strongly affect crystallization temperature, as measured from DTA analysis (onset of crystallization). Increasing of MnO content in mold flux results in a sharp decrease of Tcry due to important alterations of its crystallizing behavior. Actual nature of this phenomenon still needs some understanding [3].
In the present work, crystallization of MnO-doped and un-doped mold fluxes has been thoroughly investigated by DTA analysis at different cooling rates to understand the inherent chemical-physical effect induced by MnO.
Continuous Cooling Transformation (CCT) diagrams based on DTA data have been taken into consideration to point out the relationship between onset of crystallization and cooling rates. CCT diagrams clearly described the crystallization phenomenon as recently reported in literature [4,5]. Peculiar effect of MnO addition has been more extensively analyzed on these bases.
Calculated values of onset of crystallization obtained by extrapolation at cooling rates approaching zero have been compared with equilibrium break temperatures measured by high temperature rotational viscosimetry.

2.0 Experimental

2.1 Materials.

Experiments were carried out on powder lab sample, name 'un-doped'. Another sample, named 'doped', was obtained by mechanical mixing (home designed rotating shaker) of specific amounts of MnO (Aldrich Chem. Co., 99,99+ %) with parent 'un-doped' material. Characteristics of these samples are reported in Table 1.

2.2 Sampling.

Material samples of 1 kg have been divided into consistent samples of 100 g (Rotating Divider Retsch PK1000, Vibratory Feeder DR100/75). The small samples have been finely grained (mesh size < 100 ~ for a residue of> 99 %) by means of a rotating mill (Herzog HSM 100H) to increase the homogeneity of the final sample. The analyses have been performed on these final samples or on fractions of the same if required.

2.3 XRF Analysis.

Spectrometric analyses were carried out by means of Philips 2400 XRF spectrometer equipped with SuperQ (Ver. 2.0B) analytical software. Suitable amount of samples of material was analyzed consistently with XRF standard analytical procedure. Relevant chemical characteristics of samples are reported in Table 1. Data refer to DTA and viscosimetry pre-measurements samples analyses.

2.4 DTA Analysis.

Differential Thermal Analysis measurements were performed with L62 DTA instrument, equipped with Controller L70/215C and Data Acquisition Card L70/2001,

by Linseis GmbH. This apparatus was modified by installing a Pt-Rh sample holder for better quantitative evaluation of heat changes. Analytical procedure was as follow. Two Pt-Rh crucibles, filled with ~ 50 mg of Al_2O_3 reference material (Nabalox N0102, Nabaltech GmbH) and ~ 50 mg of powder sample, were allocated in defined position onto the stage. Crucibles were heated in the heating unit from RT to 1673 K at 10 K/min. and kept at this temperature for 10 mm. for equilibration and homogenization of the slag.
In order to ascertain dependence of crystallization temperature on cooling rate, samples were cooled from 1673 K to 573 K at different rates: 7 K/min, 13 K/min. and 20 K/min.
Recorded data were elaborated with software WIN-HDSC provided by Linseis GmbH. This software allows precise evaluation of onset point.

2.5 High temperature viscosity measurements.
High temperature viscosimetry measurements were performed with Haake Rotovisco RV2 apparatus previously calibrated by means of high temperature reference materials (NBS standard glasses with different values of viscosity). Acid cleaned crucible and rotating bob made of Pt-Rh-Ir alloy were used for each measurement.
Measurements performed on cooling cycle were taken at equilibrium within about 10 minutes.

3.0 Results

3.1 DTA Crystallization temperatures.
Onset temperatures of exothermic reaction peak in a cooling segment of DTA curves are generally defined as 'crystallization temperatures' of analyzed slag.
Onset temperatures of transformation corresponding to slag crystallization were evaluated from DTA analyses for both 'doped' and 'un-doped' samples. To obtain reliable data set, different measurements at same conditions have been performed with fresh samples and average value of resulting onset temperatures has been taken as the most accurate one. It has been observed that general dispersion of measured crystallization temperatures results as low as ~ 2%. However, in few cases more important deviations have been obtained probably due to non homogeneous or not consistent samples and unpredictable side processes or erroneous handling procedures. Results of these experiments have been discharged.

3.2 Relationship between onset point and cooling rate.
In order to study dependence of onset points on cooling rate, crystallization behavior of samples were analyzed by DTA within temperature interval from 1673 K to 573 K at different cooling rates: 7 K/min, 13 K/min. and 20 K/min.
Experimental results showed a significant variation of crystallization temperatures measured at higher cooling rates, in comparison with those measured at lower cooling rates.
Reported data confirm that onset of crystallization is a function of cooling rate. In particular, more important deviation has been evidenced for doped samples. It's possible to understand in a better way these conclusions by analyzing the data obtained by DTA at different cooling rates in terms of Continuous Cooling Transformation diagram as reported in Figure 1.
Different behavior of two materials at different cooling rates is clearly evidenced by

path of related CCT curve.

3.3 Crystallization temperatures.

In previous paragraph it has been shown that crystallization temperature, measured by DTA ($T_{Cry.}^{DTA}$), is a function of cooling rate (ν_{COOL}). Thus, 'Equation 1' follows.

Equation 1:

$$T_{Cry.}^{DTA} = \Omega(\bar{x}, \nu_{COOL})$$

Where $\bar{x}$ is the vector of all thermodynamics and kinetics parameters.

Assuming to have a DTA instrument allowing measurements at infinitely low cooling rate, i.e., carrying measurements through infinite quasi-equilibrium states, 'Equation 2' can be considered:

Equation 2:

$$\lim_{\nu_{COOL} \to 0} T_{Cry.}^{DTA} = T_{Cry.} = \Omega(\bar{x})$$

Where finally 'measured' $T_{Cry.}$ is a function of thermodynamics and kinetics parameters only.

In order to obtain a reliable estimation of $T_{Cry.}$, linear regressions of data set on Table 2 were extrapolated for $\nu_{COOL} = 0$, see Figure 2.

Calculated values are quite similar, resulting 1457 K and 1453 K for doped and un-doped sample respectively.

3.4 Viscosity Data.

Differences between doped and un-doped materials have been evidenced by high temperature viscosity measurements. Experimental viscosity data measured in a narrow value range centered on 1573 K showed good consistency with data calculated by Riboud model (based on pre-measurements chemical analysis), confirming a significant decrease of viscosity for doped sample, see Table 3.

A sharp drop of viscosity due to pick-up of MnO from steel is a well-documented phenomenon in standard casting practice of high manganese steels. Measured viscosity data, as reported in Figure 3, confirmed the expected trend, giving the idea of the extent of the difference between samples slag fluidity (η^{-1}, $poise^{-1}$).

Arrhenius plot of viscosity data set allows estimation of 'Break Temperature', T_{break}, numerically identified as the discontinuity of log η – T^{-1} curves. The physical meaning of this point is still a controversial matter. Actually, temperature where viscosity increases suddenly is sometimes referred as solidification or crystallization temperature. Therefore, due to defect of understanding, it's preferable to use given definition of T_{break}, which is unequivocal and traceable to viscosity measurements. Moreover, from a technological point of view T_{break} corresponds to the point where liquid lubrication starts to break down.

In first approximation, considering experimental data it's possible to conclude that T_{break} obtained as described above for both samples are very similar, differing only for few degrees, Δ= 22 K, see values are reported on Table 4.

4.0 Discussion.

4.1 Comparison between DTA and Viscometer analysis.

The comparison between $T_{Cry.}$ and T_{break} is provided in Table5.

Taking into account possible inaccuracy due to mathematical extrapolation fitting routines, experimental data seems to suggest that measured values are very consistent, showing a difference of less than 5% (see Table 5, δ defined as $\left(T_{Cry.} - T_{break}\right) / T_{break} \times 100$).

First consequence of these observations is that comparison between DTA and viscometer measurements when possible (i.e. in case of crystallizing slag) can be made for consistent analytical procedure: T_{break} extrapolated from viscosity equilibrium data should be compared with $T_{Cry.}^{DTA}$ extrapolated for $\nu_{COOL} = 0$. Indeed, some recent results demonstrated clearly that T_{break}, measured by dynamic viscometer analysis, decreases as the cooling rate increases probably due to supercooling of slag during measurements [6].

Then it could be concluded that with reasonable approximation:

Equation 3:

$$T_{break} \equiv T_{Cry.}$$

In this perspective, it naturally follows that T_{break} represents the point where solids are first precipitated in the melt and early nucleation occurs in case of crystallizing slag.

4.2 DTA measurements at higher cooling rate. MnO Effect.

In paragraph 3.1 some data have been discussed regarding the effect of cooling rate in measuring $T_{Cry.}^{DTA}$ and it has been stressed that more important deviations occur for doped sample. Indeed, comparing T_{break} with $T_{Cry.}^{DTA}$ measured at higher cooling rate (13÷20 K/min.) in case of doped samples, one can observes differences higher than 100K. Elsewhere, it has been shown that when all experimental parameters are kept constant, differences or gap between T_{break} and $T_{Cry.}^{DTA}$ depend on MnO content of the slag: high extent of MnO doping leads to higher gap [3].

Taking into account previous considerations it's possible to envisage a *sui generis* MnO effect on crystallization properties of the slag. Actually, it seems that MnO affects significantly crystallization kinetic of doped materials in comparison with un-doped ones. Indeed, a shift of $T_{Cry.}^{DTA}$ to lower temperatures in CCT diagram corresponds to a longer time for starting of crystallization process in a Time Temperature Transformation (TTT) diagrams.

5.0 Conclusions.

Crystallization of MnO-doped and un-doped mold fluxes at different cooling rates has been investigated to comprehend peculiar chemical-physical effects induced by this transition metal oxide. By DTA analysis relationship between onset of crystallization and cooling rate has been evidenced. Crystallization temperatures calculated by extrapolation for cooling rates approaching zero have been found quite similar to

equilibrium break temperatures determined with high temperature rotational viscosimetry.
Peculiar effect of MnO doping substantially has been targeted to consist in lowering crystallization temperature and reducing kinetics of this process (increase of time of crystallization).

6.0 References.

1. V.Ghilardi, R.Carli and G.Faravelli, 3nd *European Conf. on Continuous Casting,* Proceedings, Madrid, 1998, p.977.
2. V.Ghilardi, *unpublished results,* 1988.
3. R.Carli and V.Ghilardi, *I&SM*, ISS, 1998, Vol.25(6), p.43.
4. Y.Kashiwaya, C.E.Cicutti and A.Cramb, *ISIJ International,* ISIJ, 1998, Vol.38(4), p.357.
5. C.Orrling and A.Cramb, A.Tilliander, Y.Kashiwaya, *ISS Transactions, I&SM,* ISS, 2000, Vol.27(1), p.53.
6. S.Sridhar, K.C.Mills, O.D.C.Afrange, H.P:Lorz and R.Carli, *Ironmaking and Steelmaking,* IOM, to be published.

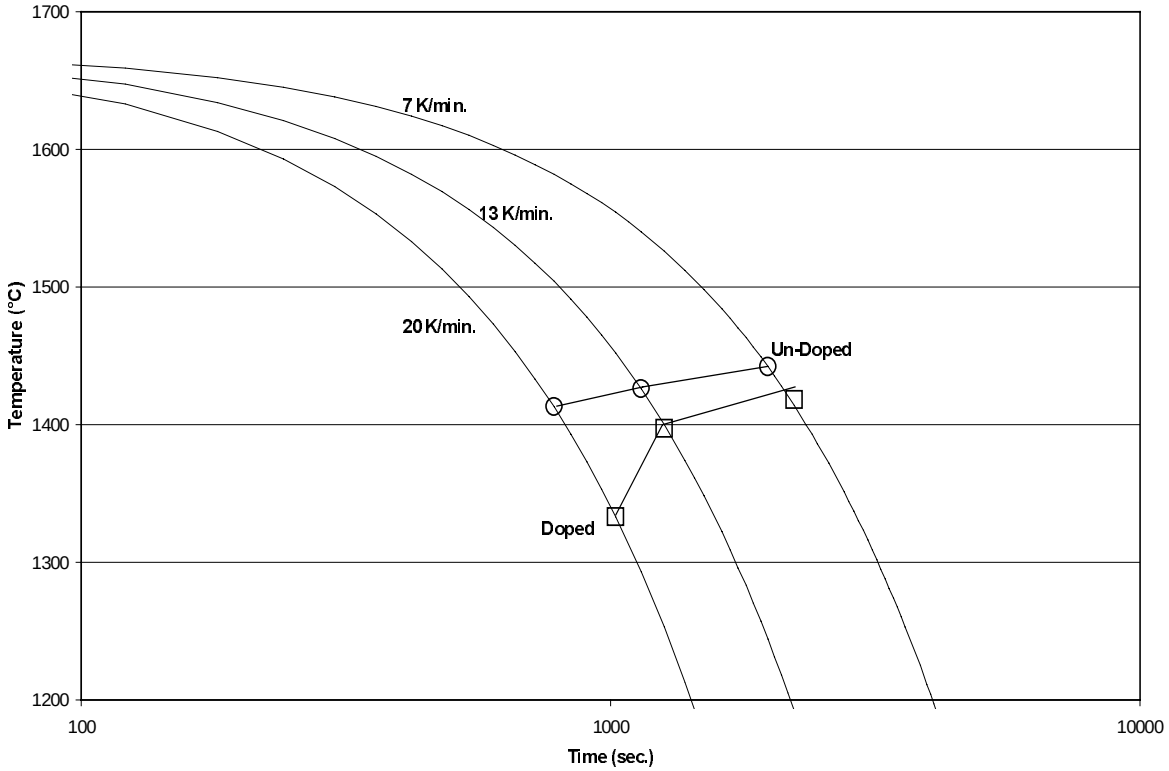

Figure 1: CCT curves.

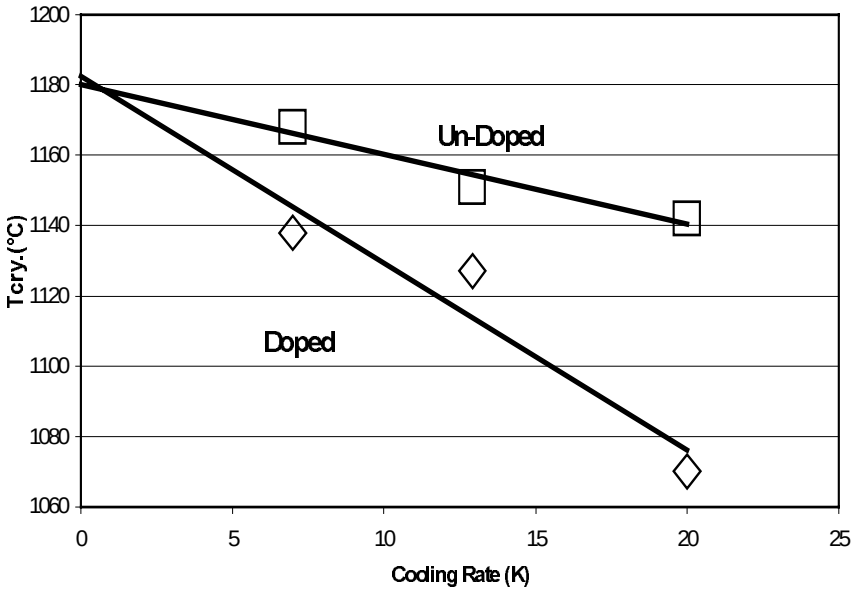

Figure 2: Extrapolation of T_{cry}.

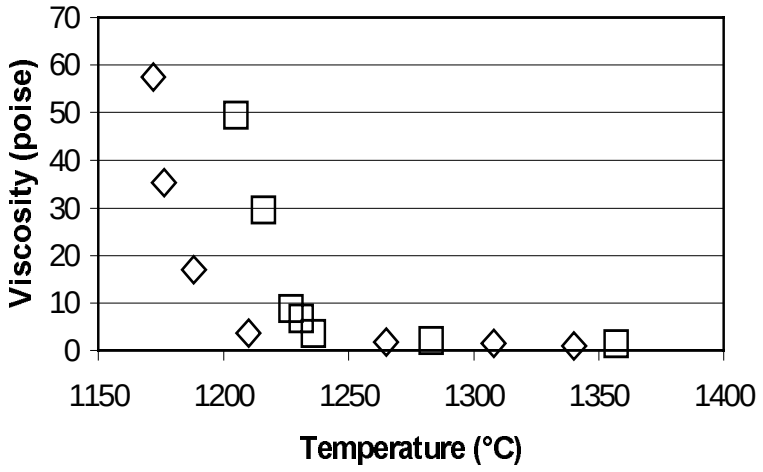

Figure 3: Measured viscosity data.

Table 1: Samples characteristics.

PROPERTIES(*)	Un-Doped	Doped
Loss of ignition (#)	17.15	15.58
C total (§)	9.15	8.63
C free (calculated)	6.19	6.06
Basicity Index (XRF analysis)	1.13	1.13
Alkali (XRF analysis)	6.02	5.88
Fluorine (XRF analysis)	5.76	5.55
MnO (XRF analysis)	/	4.99

(*) Weight percentage.
(#) In furnace at 900°C for 90 mins.
(§) Determined by Leco IR 212/CS 244 Carbon Sulphur determinator.

Table 2: Crystallization temperatures at different cooling rates.

	Crystallization Temperatures	
Cooling Rate	Doped	Un-Doped
7 K/min.	1138	1168
13 K/min.	1127	1151
20 K/min.	1070	1142

Table 3: Samples viscosity.

	Viscosity (poise)	
Origin	Doped	Un-Doped
Riboud (1573 K)	1.49	1.87
Measured	1.42 (1581 K)	2.05 (1556 K)

Table 4: Extrapolated values for T_{break}

T_{break} (K)	
Doped	Un-Doped
1490	1512

Table 5: DTA and viscometer analyses

	Doped	**Un-Doped**
T_{break}	1490	1512
$T_{Cry.}$	1457	1453
δ	2.2	4.1